Archives Italiennes de Biologie, 140: 229-236, 2002.

PRIMARY MOTOR CORTEX NEURONAL DISCHARGE DURING REACH-TO-GRASP: CONTROLLING THE HAND AS A UNIT

C.R. MASON, J.E. GOMEZ, AND T.J. EBNER*

Department of Neuroscience, University of Minnesota, 2001 Sixth St. S.E., Minneapolis, MN 55455, USA

INTRODUCTION

Reach-to-grasp is a highly complex action requiring the coordinated movements of multiple joints with over 25 degrees of freedom at the shoulder, wrist, and hand. Given this biomechanical complexity, how does the CNS control the hand during reach-to-grasp? A more traditional viewpoint has emphasized a strategy based on controlling individual muscles and joints to generate the needed forces (10, 19). Another view has emphasized the need for 'simplifying' strategies, which reduce the number of degrees of freedom and the complexity of the control problem (1, 16, 17). Recent psychophysical, anatomical, and physiological studies have found support for the latter view.

Movements of the fingers, wrist, and arm occur in a coordinated manner. Humans and non-human primates do not move individual fingers in isolation of neighboring fingers, even when that is the explicit goal (20). In typing and piano playing, almost all fingers and joints are in motion simultaneously (4, 24). Hand shape evolves throughout the reach and is highly dependent on object properties (8, 13, 14) and is temporally coupled to the arm movement (3, 14). Only a few postural synergies are needed to describe static hand shape (16) or the hand shape throughout reach-to-grasp (13). Therefore, global control strategies may be used to coordinate movements of the arm and hand.

The primary motor cortex (M1) is not organized simply to control individual muscles. Focal stimulation elicits movements of multiple digits and contraction of a particular hand muscle can be evoked from a substantial fraction of M1 (19). A single corticomotoneuron facilitates the activity of multiple muscles (2, 11). Focal inactivations in the monkey M1 hand region and small strokes in humans disrupt movements of multiple fingers, not movements of isolated fingers (18, 22). Single M1 neurons discharge with movements of multiple fingers and neurons modulated by different fingers movements overlap extensively (6, 15, 21). Therefore, a neuronal substrate exists in M1 consistent with global control of the hand and fingers. This study tests the hypothesis that aspects of hand/object shape are represented in the discharge of M1 neurons, reflecting control of the hand as a unit. Previous single unit recordings in M1 focused on the modulation of M1 neurons during isometric pinch tasks (12, 23) or individual finger movements (15, 21), not reach-to-grasp.

*Address for correspondence. - Dr. T.J. Ebner, Department of Neuroscience, University of Minnesota, Lions Research Bldg, Rm. 421, 2001 Sixth St. S.E., Minneapolis, MN 55455. Tel. 612 626 2205, Fax: 612 626 9201, Email: ebner001@umn.edu

METHODS

Two rhesus monkeys were trained to reach and grasp objects with an overhand power grasp using specific force levels. The animals viewed a computer monitor which displayed a timing square and a force window that signaled the required force and the force feedback. The animals began the task by placing their right hand on a start plate, exerting a force for a randomized period (1-1.5 s). The timing square signaled the animal to reach (15 cm) and grasp the target object. During the static grasp period the animals were required to maintain specified grasp force for at least 1.5 s.

Sixteen objects in four classes were presented in a pseudorandom block design: I) 4 cubes, II) 5 rectangular solids, III) 4 multi-sided polygonal prisms and IV) 3 cylinders. Within a class the objects varied in shape, volume, and/or orientation. The animals were also required to exert 5 different levels of anterior-posterior (AP) grasp force (0.1 - 0.3, 0.3 - 0.5, 0.5 - 0.7, 0.7 - 0.9, 0.9 - 1.1 Newtons).

The positions of monkeys' wrists, hands and fingers in 3 dimensions were recorded using a video-based motion analysis system. Twelve reflective markers were used including a marker: 1) proximal to the dorsal wrist crease, 2) at the dorsal wrist crease, 3) at each long finger metacarpophalangeal (MCP) and distal interphalangeal joints (DIPs) and 4) at the thumb MCP and interphalangeal joint (IP). The markers were monitored with 6 cameras, digitized (60 Hz), and tracked throughout the reach-to-grasp.

After training, the animals were prepared for chronic single cell recordings including a chamber over the left M1 and a head fixation system (5). Single neurons were recorded extracellularly, discriminated, and stored for analyses if their discharge modulated audibly during task performance (5). Receptive fields of each unit were examined by somatosensory stimulation and passive movements (5). To identify the hand areas of M1 and the M1/dorsal premotor cortex (PMd) boundary, intracortical microstimulation (ICMS) was performed following many of the recording sessions using established protocols (25), monitoring the threshold of evoked muscle contractions.

Analysis

The task was divided into four periods for the kinematic analyses: 1) initial hold period which ended with lift off from the start pad, 2) reach period and 3) early grasp period which began at AP force initiation and 4) static grasp period with maintained force. Because the reach duration was not constant, the reach periods were normalized to a 1 sec duration using a spline interpolation procedure and then concatenated with the initial hold and grasp periods. The normalized kinematic data were then averaged across each object/force combination, calculating the means and standard deviations of the wrist path and speed to test for similarities/differences in the reaches.

This experiment was designed to test whether object properties (which co-vary with hand shape) and grasp force are encoded in the discharge of neurons in the M1 hand area. An initial "object-based" temporal regression model (eqn. 1) evaluated how the discharge was correlated with the objects in time. The firing, F, in each 20 msec bin (t_i) was regressed to the objects (OB) and grasp force (f) level the monkey was required to maintain.

$$F(t_i) = \beta_o(t_i) + \beta_{force}(t_i)f + \sum_{k=1}^{16} \beta_{object_k}(t_i)OB_k \qquad \text{(eqn. 1)}$$

The objects were condensed into a single dummy-variable classification: object (OB).

A second "attribute-based" regression model (eqn. 2) was used that related the firing to specific object properties and grasp force (f). The 3 properties chosen were object volume (V), class (C), and orientation (O). Specifically, the model was:

$$F(t_i) = \beta_0(t_i) + \beta_{force}(t_i)f + \beta_{volume}(t_i)V + \sum_{j=1}^{4} \beta_{class_j}(t_i)C_j + \sum_{k=1}^{4} \beta_{orientation_k}(t_i)O_k \qquad \text{(eqn. 2)}$$

Force and object volume (f and V, respectively) were included as numeric data and object class (C_1-C_4) and object orientation (O_1-O_4) as dummy variables. Object orientations were based on the orientation of the object's major axis along one of the three Cartesian axes. Cubes had no single major axis and were placed into the null category.

To compare the two models, it was critical to adjust for the differences in the number of parameters. Therefore, the adjusted-R^2 statistic, was calculated:

$$\overline{R}^2 = 1 - \left(\frac{n-1}{n-p}\right)(1-R^2) \qquad \text{(eqn. 3)}$$

with n the number of sample, p the number of parameters, and R^2 the coefficient of determination for the different models.

These experiments were approved and monitored by the University of Minnesota's Institutional Animal Care and Use Committee.

RESULTS

Reach-to-grasp behavior.

The animals performed the task using the required grasp force (Fig. 1A). Several analyses evaluated the dependence of the grasp force and reach kinematics on the objects. First, the static grasp force as well as the rate of force production did not vary as a function of the object for a given force level (ANOVA, $P > 0.05$, F-test). However, as expected the higher force levels were associated with a higher rate of force production (ANOVA, $P < 0.05$, F-test). Therefore, force production was similar for each object for a given force level. Second, the reach paths were highly consistent among the various object classes and among the individual objects. Analysis of the wrist position as various times in the trial revealed no significant effects by object class (ANOVA, $P > 0.05$, F-test). Third, the tangential velocity profiles were very similar and neither the force nor object class affected peak velocity or time to peak velocity (ANOVA, $P > 0.05$, F-test). Therefore, any change in the discharge modulation was independent of the reach kinematics, and can be attributed to the different objects or grasp force.

Hand shape was also similar for the 5 force levels as determined by visual inspection of the reconstructed hands. There was an orderly progression in hand shape from an initial open hand configuration to the object grasp that was qualitatively similar from the lowest to the highest force windows. Therefore, force and hand shape were relatively independent and contributed to the discharge modulation separately.

Discharge characteristics of single cells.

A total of 120 M1 cells were recorded (71 neurons in monkey G and 49 in monkey L). This report analyzed 58 cells in which the monkeys completed trials to 8 or more objects at 5 force levels. The ICMS results were consistent with the cells being located in M1. Although the cells had a variety of response patterns, discharge modulation was prominent during the reach and the grasp periods and varied with the objects and force requirements.

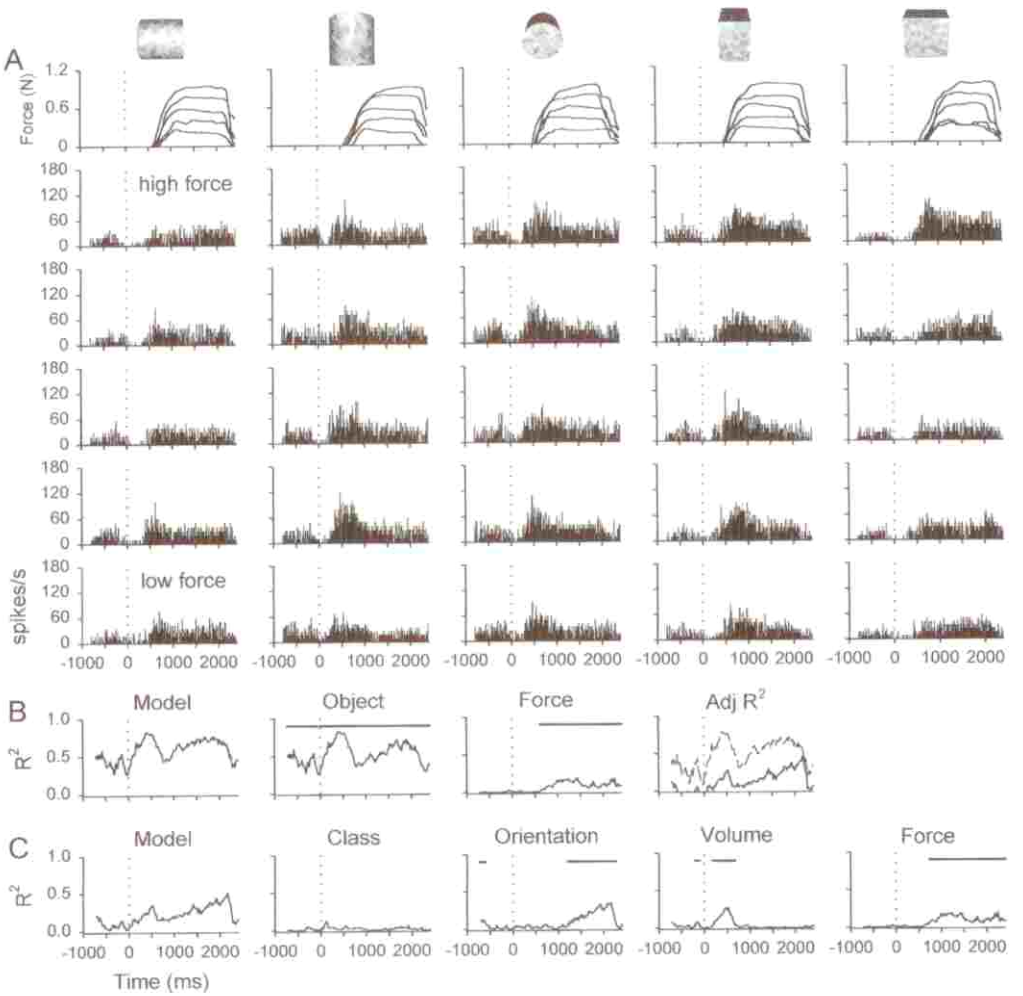

Fig. 1. - *Example of a M1 cell with increased firing during grasp.*
A. The force levels and spike firing histograms during reach-to-grasp of the depicted objects suggested a relationship to object orientation and force requirements. Each force trace and histogram is the average of 5 trials aligned on movement onset (dotted vertical line). Each row represents a different force level from high (top) to low (bottom). B. Results of the object-based regression based on responses across 18 objects including 3 repeats and 5 force levels and the comparison of the adjusted R^2 of the two models. Significant correlations (ANOVA, $P < 0.05$) of 5 or more consecutive bins in the partial R^2 plots are indicated by the bars above the plots. The partial R^2 for object reflected the correlations observed for the R^2 of the object properties in the attribute-based regression. In the adjusted R^2 graph, the solid line represents the attribute-based model and the dashed line the object-based model. C. Model and partial R^2 plots from the attribute-based regression based on the responses to same objects and force levels as above. This neuron's discharge was modulated by volume at the end of the reach and early grasp. Modulation to object orientation and force occurred during static grasp.

Figure 1A illustrates a cell with discharge modulation during reach and grasp. Initially, the firing decreased then increased during the reach and in early grasp. The

discharge modulation during grasp was highly dependent on the object orientation and was greatest for the cylinder (the middle column) and for the rectangular solid (column 4) with their long axes oriented sagittally. It was least for the objects presented parallel to monkeys' frontal plane. The discharge was also modulated by the task force requirements, best illustrated by the 2 rectangular solids in which higher force was correlated with increased firing (columns 4 and 5).

The object-based regression analysis confirmed that the objects (and by inference hand shape) explained a large fraction of the firing variability (Fig. 1B) accounting for 83% of the variability. The cell firing was also correlated to force. The attribute-based regression showed that object volume and orientation were also significant predictors (Fig. 1C). The significant correlation to volume occurred first during the reach and early grasp and is evident in the burst of activity for the two objects with sagittal orientation. The object volume enclosed by the monkey's hand was greatest in this orientation and this peak may reflect the greater hand opening to grasp these objects. The significant correlation to orientation and force occurred later during static grasp with force explaining approximately 18.5% of the firing variability. As expected, the partial R^2 for force was identical to the object-based model. Therefore, the modulation of firing during the reach and grasp was highly dependent on the object properties including volume and orientation.

The object-based regression results for the population indicate that the firing was correlated with the objects throughout the four task periods (Fig. 2). Discharge modulation was most prominent during the reach but significant correlations to class, orientation and volume were common during reach, early and static grasp. In contrast,

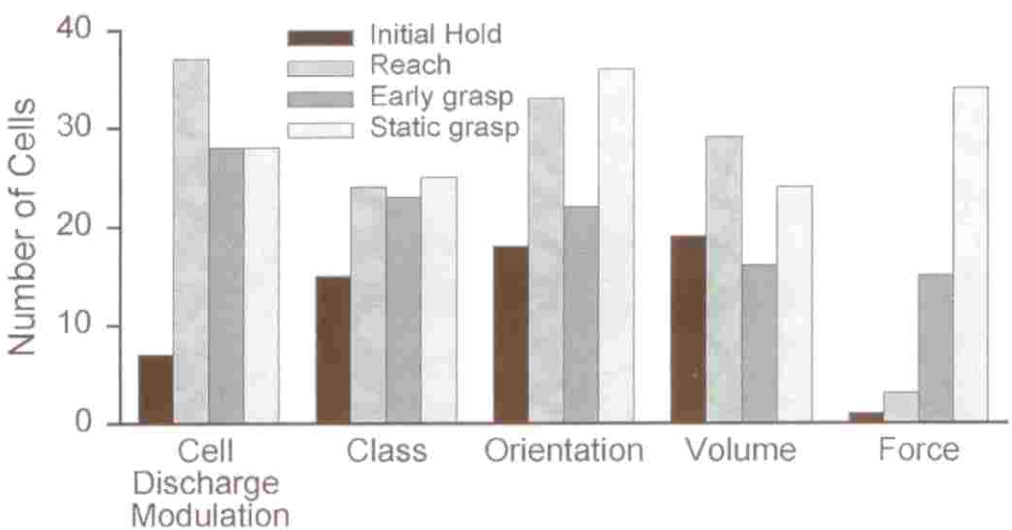

Fig. 2. - *Histogram showing periods of cell discharge modulation and significant correlations to the object parameters as a function of the four task periods.*
The peak number of cells were modulated during reach. A large fraction of cells has significant correlations with the object properties during reach and grasp periods. Correlations to force were present primarily during early and static grasp. A cell could be counted in multiple columns.

correlations to force were not uniform, with little force related modulation during the reach and the most during static grasp.

DISCUSSION

The study's primary goal was to evaluate whether, and if so how, hand posture/object properties and grasp force modulate the discharge of MI neurons. To achieve that goal, the paradigm must avoid correlations between hand posture and either force or the kinematics of reach. The task design minimized reach variability since the start and target locations were constant and independently varied object properties and force. These parameters were, therefore, orthogonal by definition. The kinematic analysis confirmed that wrist path and its speed profile were highly stereotypic for the different object classes and did not depend on the task force requirements. Therefore, the variation in neuronal discharge observed with the different objects and force levels was not a function of reach. The lack of coupling assures that the object related parameters and the force parameters used in the various regression models are relatively independent and colinearity in the predictors was not a problem and that the kinematics of the reach, which was not specifically included in the models, was not a major confound.

The modulation patterns occurring in both the reach and the grasp periods suggest that the global parameters of reach-to-grasp are represented in the discharge of M1 neurons. Over half the cells (68.3%) changed their firing rate during reach. This early modulation is hypothesized to reflect the hand shaping in preparation for the grasp (3, 13, 14, 17). Given that the reach was constant over object classes and force levels, this modulation is likely related to the hand shaping, as the regression results suggest. A large fraction of the cells were also modulated during the two grasp periods (67.2%). The correlations with object properties during early grasp and static grasp likely reflect the hand shape as it conformed to the object.

Correlations with force were also observed, consistent with previous pinch studies (12, 23). However, the force related modulation was not the major predictor. Force modulation was most prominent during grasp, consistent with the concept that movement parameters are encoded as needed (9). The strong modulation during the reach that was highly dependent on the objects demonstrates that these cells are not limited to signaling force.

The observation that the discharge modulation was a function of object properties, while consistent with our hypothesis of a global representation of grasp (1, 16, 17), does not differentiate between whether extrinsic or intrinsic aspects of hand shape are represented. Hand shape and object highly co-vary both for monkeys (7) and human grasps (13). The object- and attribute-based regression results reveal that the objects explain a greater amount of the firing variability than did our arbitrarily selected object attributes. Furthermore, as the adjusted R^2 shows, the increase was not simply a consequence of the increase in the number of parameters in the model (Fig. 1B). We hypothesize that intrinsic measures of hand shape may explain some of that additional firing variability.

SUMMARY

This study has begun to test the hypothesis that aspects of hand/object shape are represented in the discharge of primary motor cortex (M1) neurons. Two monkeys were trained in a visually cued reach-to-grasp task, in which object properties and grasp forces were systematically varied. Behavioral analyses show that the reach and grasp force production were constant across the objects. The discharge of M1 neurons was highly modulated during the reach and grasp. Multiple linear regressions models revealed that the M1 discharge was highly dependent on the object grasped, with object class, volume, orientation and grasp force as significant predictors. These findings are interpreted as evidence that the CNS controls the hand as a unit.

REFERENCES

1. ARBIB, M.A., IBERALL, T., AND LYONS, D. Coordinated control programs for movements of the hand. *Exp Brain Res.*, **10**: 111-129, 1985.
2. CHENEY, P.D. AND FETZ, E.E. Comparable patterns of muscle facilitation evoked by individual corticomotoneuronal (CM) cells and by single intracortical microstimulation in primates: evidence for functional groups of CM cells. *J Neurophysiol.*, **53**: 786-804, 1985.
3. CHIEFFI, S. AND GENTILUCCI, M. Coordination between the transport and the grasp components during prehension movements. *Exp. Brain Res.*, **94**: 471-477, 1993.
4. ENGEL, K.C., FLANDERS, M., AND SOECHTING, J.F. Anticipatory and sequential motor control in piano playing. *Exp. Brain Res.*, **113**: 189-199, 1997.
5. FU, Q-G., SUAREZ, J.I., AND EBNER, T.J. Neuronal specification of direction and distance during reaching movements in the superior precentral premotor area and primary motor cortex of monkeys. *J. Neurophysiol.*, **70**: 2097-2116, 1993.
6. GEORGOPOULOS, A.P., PELLIZZER, G., POLIAKOV, A.V., AND SCHIEBER, M.H. Neural coding of finger and wrist movements. *J. Comput. Neurosci.*, **6**: 279-288, 1999.
7. GOMEZ URANGA, J.E. *Reach to Grasp Representations in the Monkey Motor Cortex: Endpoint Accuracy and Grasp Posture*. Ph.D. Dissertation, University of Minnesota, 2000.
8. JEANNEROD, M. The timing of natural prehension movements. *J. Motor. Behav.*, **16**: 235-254, 1984.
9. JOHNSON, M.T.V., MASON, C.R., AND EBNER, T.J. Central processes for the multiparametric control of arm movements. *Curr Opin Neurobiol*, **11**: 684-688, 2001.
10. LEMON, R.N. Neural control of dexterity: what has been achieved? *Exp Brain Res.* **128**: 6-12, 1999.
11. LEMON, R.N., MANTEL, G.W., AND MUIR, R.B. Corticospinal facilitation of hand muscles during voluntary movement in the conscious monkey. *J. Physiol., Lond.*, **381**: 497-527, 1986.
12. MAIER, M.A., BENNETT, K.M.B., HEPP-REYMOND, M.C. AND LEMON, R.N. Contribution of the monkey corticomotoneuronal system to the control of force in precision grip. *J. Neurophysiol.*, **69**: 772-785, 1993.
13. MASON, C.R., GOMEZ, J.E., AND EBNER, T.J. Hand synergies during reach-to-grasp. *J Neurophysiol.*, **86**: 2896-2910, 2001.
14. PAULIGNAN, Y., MACKENZIE, C., MARTENIUK, R., AND JEANNEROD, M. The coupling of arm and finger movements during prehension. *Exp. Brain Res.*, **79**: 431-435, 1990.

15. POLIAKOV, A.V. AND SCHIEBER, M.H. Limited functional grouping of neurons in the motor cortex hand area during individuated finger movements: a cluster analysis. *J. Neurophysiol.*, **82**: 3488-3505, 1999.
16. SANTELLO, M., FLANDERS, M., AND SOECHTING, J.F. Postural hand synergies for tool use. *J. Neurosci.*, **18**: 10105-10115, 1998.
17. SANTELLO, M. AND SOECHTING, J.F. Gradual molding of the hand to object contours. *J. Neurophysiol.*, **79**: 1307-1320, 1998.
18. SCHIEBER, M. Somatotopic gradients in the distributed organization of the human primary motor cortex hand area: evidence from small infarcts. *Exp. Brain Res.*, **128**: 139-148, 1999.
19. SCHIEBER, M.H. How might the motor cortex individuate movements? *Trends Neurosci.*, **13**: 440-445, 1990.
20. SCHIEBER, M.H. Individuated finger movements of Rhesus monkeys: a means of quantifying the independence of the digits. *J. Neurophysiol.*, **65**: 1381-1391, 1991.
21. SCHIEBER, M.H. AND HIBBARD, L.S. How somatotopic is the motor cortex hand area? *Science.*, **261**: 489-492, 1993.
22. SCHIEBER, M.H. AND POLIAKOV, A.V. Partial inactivation of the primary motor cortex hand area: effects of individuated finger movements. *J. Neurosci.*, **18**: 9038-9054, 1998.
23. SMITH, A.M., HEPP-REYMOND, M.C., AND WYSS U.R. Relation of activity in precentral cortical neurons to force and rate of force change during isometric contractions of finger muscles. *Exp. Brain Res.*, **23**: 315-332, 1975.
24. SOECHTING, J.F. AND FLANDERS, M. Flexibility and repeatability of finger movements during typing: analysis of multiple degrees of freedom. *J. Comput. Neurosci.*, **4**: 29-46, 1997.
25. WEINRICH, M. AND WISE, S.P. The premotor cortex of the monkey. *J. Neurosci.*, **2**: 1329-1345, 1982.